Published OnlineFirst March 31, 2014; DOI: 10.1158/1078-0432.CCR-13-1246

Clinical Cancer Research

Zoledronic Acid Has Differential Antitumor Activity in the Pre- and Postmenopausal Bone Microenvironment *In Vivo*

Penelope D. Ottewell, Ning Wang, Hannah K. Brown, et al.

Clin Cancer Res 2014;20:2922-2932. Published OnlineFirst March 31, 2014.

Published OnlineFirst March 31, 2014; DOI: 10.1158/1078-0432.CCR-13-1246

Clinical Cancer Research

Cancer Therapy: Preclinical

See related article by Wright and Guise, p. 2817

Zoledronic Acid Has Differential Antitumor Activity in the Pre- and Postmenopausal Bone Microenvironment *In Vivo*

Penelope D. Ottewell[1], Ning Wang[2], Hannah K. Brown[1], Kimberly J. Reeves[2], C. Anne Fowles[2], Peter I. Croucher[3], Colby L. Eaton[2], and Ingunn Holen[1]

Abstract

Purpose: Clinical trials in early breast cancer have suggested that benefits of adjuvant bone-targeted treatments are restricted to women with established menopause. We developed models that mimic pre- and postmenopausal status to investigate effects of altered bone turnover on growth of disseminated breast tumor cells. Here, we report a differential antitumor effect of zoledronic acid (ZOL) in these two settings.

Experimental design: Twleve-week-old female Balb/c-nude mice with disseminated MDA-MB-231 breast tumor cells in bone underwent sham operation or ovariectomy (OVX), mimicking the pre- and postmenopausal bone microenvironment, respectively. To determine the effects of bone-targeted therapy, sham/OVX animals received saline or 100 μg/kg ZOL weekly. Tumor growth was assessed by *in vivo* imaging and effects on bone by real-time PCR, micro-CT, histomorphometry, and measurements of bone markers. Disseminated tumor cells were detected by two-photon microscopy.

Results: OVX increased bone resorption and induced growth of disseminated tumor cells in bone. Tumors were detected in 83% of animals following OVX (postmenopausal model) compared with 17% following sham operation (premenopausal model). OVX had no effect on tumors outside of bone. OVX-induced tumor growth was completely prevented by ZOL, despite the presence of disseminated tumor cells. ZOL did not affect tumor growth in bone in the sham-operated animals. ZOL increased bone volume in both groups.

Conclusions: This is the first demonstration that tumor growth is driven by osteoclast-mediated mechanisms in models that mimic post- but not premenopausal bone, providing a biologic rationale for the differential antitumor effects of ZOL reported in these settings. *Clin Cancer Res; 20(11); 2922–32. ©2014 AACR.*

Introduction

There is increasing evidence of differential therapeutic effects of bone-sparing agents in the pre- and postmenopausal setting from clinical trials in breast cancer, with benefits largely confined to women with established menopause (1–3). These results indicate that the mechanisms that govern breast cancer progression, and also the response to therapeutic intervention, are influenced by the endocrine status of the patient. The first indication that menopausal status was important in determining the response to antiresorptive agents came from the AZURE (Does Adjuvant Zoledronic acid redUce REcurrence in stage II/III breast cancer?) trial (1). In AZURE, 3,360 women at high risk of breast cancer recurrence were randomized to receive either placebo or intensive treatment with zoledronic acid (ZOL), in addition to standard therapy, and the primary endpoint was diseases-free survival (DFS). The initial analysis that included the entire study population showed no overall increase in DFS following ZOL treatment. However, subgroup analysis demonstrated that women who were postmenopausal for at least 5 years before study entry had a significantly reduced risk of DFS (25%) and the risk of death from any cause was reduced by 26%. Similar differential effects between pre- and postmenopausal patient populations have subsequently been reported from other trials, including NSABP-B34 (increased DFS in women more than age 50 receiving clodronate; ref. 2) and ABCSG-12 (increased survival in women more than age 40 who receive ZOL; ref. 3). Surprisingly, these bone-targeted agents also reduced the risk of extraskeletal recurrence, indicating that modifying the bone microenvironment affects subsequent tumor progression in distant sites.

During metastasis, the spread of breast tumor cells from the primary site to specific niches in the bone marrow is generally accepted to be an early event, and metastases may originate from these disseminated tumor cells. Once

Authors' Affiliations: [1]Academic Unit of Clinical Oncology, Department of Oncology, [2]Academic Unit of Bone Biology, Department of Human Metabolism, University of Sheffield, Sheffield, United Kingdom; and [3]Musculoskeletal Medicine Division, Garvan Institute of Medical Research, Sidney, New South Wales, Australia

Note: Supplementary data for this article are available at Clinical Cancer Research Online (http://clincancerres.aacrjournals.org/).

Corresponding Author: Penelope Ottewell, Academic Unit of Clinical Oncology, Medical School, University of Sheffield, Beech Hill Road, Sheffield, S10 2RX, UK. Phone: 44-0-114-271-2133; Fax: 44-0-114-271-1711; E-mail: P.D.Ottewell@sheffield.ac.uk

doi: 10.1158/1078-0432.CCR-13-1246

Published OnlineFirst March 31, 2014; DOI: 10.1158/1078-0432.CCR-13-1246

Translational Relevance

Our study addresses the surprising findings from clinical trials that addition of zoledronic acid (ZOL) to standard chemotherapy and/or hormone therapy has differential effects depending on the menopausal status of the patients, with the survival benefits being restricted to patients with established menopause. Our study provides the first comprehensive *in vivo* evidence of how the cellular mechanisms involved in initiating bone metastasis differ in the pre- and postmenopausal bone microenvironment. Our data also demonstrate a link between menopausal status and the differential antitumor effects of ZOL. We show that osteoclast-mediated mechanisms are instrumental in the tumorigenic progression of disseminated breast cancer cells in bone exclusively in the postmenopausal setting; providing the biologic evidence that support specific benefits of adjuvant antiresorptive therapy for postmenopausal patients with breast cancer.

established in putative metastatic niches in bone, tumor cells can remain dormant for several years under the control of environmental cues, and in many cases never develop into clinically overt metastasis (4, 5). During this period, there is a close association between tumor cells and the main cell types of the bone microenvironment, bone forming osteoblast, and bone resorbing osteoclasts (6). Eventually, yet to be identified events trigger the escape of tumor cells from dormancy, and initiate tumor progression and the development of overt bone metastasis. Modification of the bone microenvironment has been shown to affect the levels of tumor cell colonization (7). Evidence from model systems demonstrated that expansion of the osteoblast niche by administration of parathyroid hormone (PTH) increased subsequent colonization of bone by prostate cancer cells (7). The osteoclast is also key to tumor progression in bone, as pretreatment with antiresorptive agents inhibits subsequent breast tumor growth in bone and delays the progression of established tumors (8). To optimize tumor engraftment, the majority of xenograft models of bone metastasis use young animals (5–6-week-old) with an immature skeleton and rapid bone remodeling, supporting the notion that increased osteoclast activity and/or bone turnover facilitates skeletal tumor cell colonization and progression. In agreement with this, studies from model systems have demonstrated that antiresorptive agents (mainly ZOL) also inhibit development of bone metastasis in young animals (9). However, the majority of patients who develop breast cancer bone metastasis will have undergone menopause, and for this group the clinical relevance of data obtained using standard xenograft models is limited. This study is the first to establish how breast tumor cells grow bone in models that mimic the pre- and postmenopausal bone microenvironment, and to demonstrate that the potent antiresorptive agent ZOL differentially modifies tumor growth in these two settings.

Materials and Methods

Cell culture

Low passage (<P10) human breast cancer cells, MDA-MB-231-luc2 tdTomato (authenticated and purchased from Caliper Lifer Sciences) or MDA-MB-231 (European Collection of Cell Cultures) transfected with eGFP were used. Before *in vivo* inoculation eGFP-expressing cells were incubated for 15 minutes with 25 μmol/L of 1,1′-dioctadecyl-′, 3′-tetramethylindodicarbocyanine, 4-chlorobenzenesulfonate (DiD; Life Technologies). Tumor growth was monitored using an *in vivo* imaging system (IVIS) (luminol) system (Caliper Life Sciences; luc2) or an Illumatool Lighting System (LightTools Research; eGFP).

In vivo studies

We used 12-week-old female Balb/c nude mice (Charles River Laboratories). Experiments were carried out in accordance with local guidelines and with Home Office approval under project licence 40/3462, University of Sheffield, Sheffield, UK.

Following ovariectomy (OVX) or sham operation animals were sacrificed 1 to 8 weeks later ($n = 5$/group) and bone effects assessed. Effects of OVX on tumor cell homing and colonization of bone were established by OVX/sham-operating mice 7 days before tumor cell inoculation ($n = 10$/group). For studies of bone homing and colonization mice were culled 24 hours and 8 weeks after tumor cell injection, respectively. Effects of OVX on disseminated tumor cells were assessed following injection of breast cancer cells 7 days before OVX, sham, or nonoperation ($n = 10$/group) in estrogen receptor (ER)–positive and ER-negative cell lines. A total of 1×10^5 DiD-labeled MDA-MB-231-luc-2 tdTomato cells were injected into the left cardiac ventricle (intracardially), tumor growth was monitored for 8 weeks. Saline (0.1 mL) or 1×10^5 MCF7 cells were injected intracardially 4 days following sham or implantation of 17β estradiol pellet (innovative Research of America). Effects of estradiol alone were assessed at 4 weeks and tumor growth monitored for 10 weeks.

Effects of ZOL on OVX-induced tumor growth were investigated in mice inoculated with 1×10^5 DiD-labeled MDA-MB-231-eGFP cells intracardially, and given weekly ZOL (100 μg/kg) or saline ($n = 20$/group) from day 5. Seven days following tumor cell inoculation, animals from both groups underwent either sham or OVX ($n = 10$). Assessment of parathyroid hormone (PTH) on tumor growth was investigated in mice inoculated with 1×10^5 MDA-MB-231-luc-2 tdTomato cells intracardially, and given PTH (80 μg/kg) or saline daily for 5 days ($n = 10$/group) and animals sacrificed at 5 weeks.

Serum was stored at −80°C for ELISA, tibiae and femurs were fixed in 4% paraformaldehyde (PFA) for microcomputed tomograpgy (micro-CT) analysis before decalcification in 1% PFA/0.5% EDTA and processing for histology. Bones for two-photon analysis were stored in optimum cutting temperature compound (OCT) at −80°C.

Published OnlineFirst March 31, 2014; DOI: 10.1158/1078-0432.CCR-13-1246

Microcomputed tomograpgy imaging

Microcomputed tomography analysis was carried out using a Skyscan 1172 X-ray–computed microtomography scanner (Skyscan) equipped with an X-ray tube (voltage, 49 kV; current, 200 μA) and a 0.5-mm aluminium filter. Pixel size was set to 5.86 μm and scanning initiated from the top of the proximal tibia as previously described (10).

Bone histology and measurement of tumor volume

Osteoclasts were detected by toluidine blue and tartate-resistant acid phosphatase (TRACP) staining as previously described (11). Osteoblasts were identified as mononuclear, cuboidal cells residing in chains along the bone surface. The number of osteoclasts/osteoblasts per millimeter of cortical-endosteal bone surface and trabecular bone surfaces and the proportion of bone surface occupied by osteoclasts/osteoblasts was determined using a Leica RMRB upright microscope and OsteoMeasure software (Osteometrics Inc.) as previously described (12).

Two-photon microscopy

Tibiae were imaged using a multiphoton confocal microscope (LSM510 NLO upright; Zeiss). DiD-labeled cells were visualized using a 900-nm Chameleon laser, bone was detected using the 633-nm multiphoton laser (Coherent) and images were reconstructed in LSM software version 4.2 (Zeiss).

Biochemical analysis

Serum concentrations of TRACP 5b, P1NP, and PTH were measured using commercially available ELISA kits: MouseTRAP Assay (Immunodiagnostic Systems), the Rat/Mouse P1NP Competitive Immunoassay Kit (Immunodiagnostic Systems), and Mouse PTH (Uscn Life Sciences), respectively.

Real-time PCR

Gene expression was analyzed on three custom-made microarray plates (Ref, 0186817032) per group (all reagents from Applied Biosystems): Relative mRNA expression compared with the housekeeping gene glyceraldehyde-3-phosphate dehydrogenase (Hs99999905_m1) was assessed using an ABI 7900 PCR System (PerkinElmer) and TaqMan universal master mix. Fold change in gene expression between treatment groups was assessed by directly inserting C_t values into Data Assist V3.01 software (Applied Biosystems) and changes in gene expression were only analyzed for genes with a C_t value of $\leq$25.

Statistical analysis

Statistical analysis was by one-way ANOVA followed by the Newman–Keuls multiple comparison test. Statistical significance was defined as a P value of less than or equal to 0.05. All P values are two-sided.

Results

Characterization of ovariectomy-induced changes in the bone microenvironment

A longitudinal study was performed to establish how OVX modified the bone microenvironment in Balb/c nude mice (Fig. 1). Ovariectomized animals had significantly reduced trabecular bone volume by week 2, compared with sham-operated animals ($P < 0.01$), associated with an initial increase in the serum levels of the osteoclast marker TRACP, and corresponding decrease in the osteoblast activity marker P1NP. There was no significant difference in either osteoblast or osteoclast numbers between sham and OVX animals at any time point. In subsequent experiments tumor cells were inoculated 7 days following OVX for tumor cell colonization to coincide with bone loss. The bone microenvironment following sham or OVX was considered to model the pre- and postmenopausal setting, respectively.

Effects of ovariectomy on homing of breast tumor cells and colonization of bone

Tumor growth in bone was investigated following intracardiac injection of MDA-MB-231 breast cancer cells in female mice. In pilot studies, 90% of 6-week-old animals had detectable skeletal tumor growth following this protocol (Supplementary Fig. S1), compared with only 20% of 12-week-old animals, a difference attributed to the higher rate of bone turnover in young animals.

We investigated whether the OVX-induced changes to the bone microenvironment modified the ability of breast cancer cells to home to and colonize bone. MDA-MB-231 cells were injected into 12-week-old mice 7 days after OVX or sham operation. Twenty-four hours after tumor cell injection flow cytometric analysis of cells flushed from the marrow cavity of long bones showed significantly higher numbers of tumor cells in control mice compared with OVX animals [427.7 ± 87.6 tumor cells/1×10^6 mononuclear in control vs. 150.7 ± 23.17 in OVX mice ($P < 0.005$; Supplementary Fig. S2A)], implying that OVX decreases the initial number of tumor cells that home to the bone microenvironment. Multiphoton analysis of the bones confirmed these results (Supplementary Fig. S2B). Forty-eight days following tumor cell injection tumor growth in bone was detected in 17% of control and 18% of sham-operated animals, compared with 89% of animals that had undergone OVX ($P < 0.001$ for OVX vs. control or sham, Fig. 2). Number and size of tumors in the long bones were increased following OVX, with 1.67 ± 0.41 tumors detected per mouse with an average bioluminescence (BIL) of $1.09 \times 10^6 \pm 0.09 \times 10^6$ photons per second (p/s) following OVX compared with 0.43 ± 0.12 tumors with an average BIL of $0.23 \times 10^6 \pm 0.08 \times 10^6$ p/s following sham operation ($P < 0.001$). Tumor burden in non-bone sites was similar in all groups (18% in OVX, 17% in control, and 18% in sham). OVX induced the expected reduction in bone volume compared with sham/control (BV/TV $= 9.11 \pm 0.32\%$ in OVX, $13.85 \pm 0.23\%$ in control, and $14.07 \pm 0.13\%$ in sham; $P < 0.001$ for OVX vs. control or sham), supporting that modification of the bone microenvironment is associated with

Published OnlineFirst March 31, 2014; DOI: 10.1158/1078-0432.CCR-13-1246

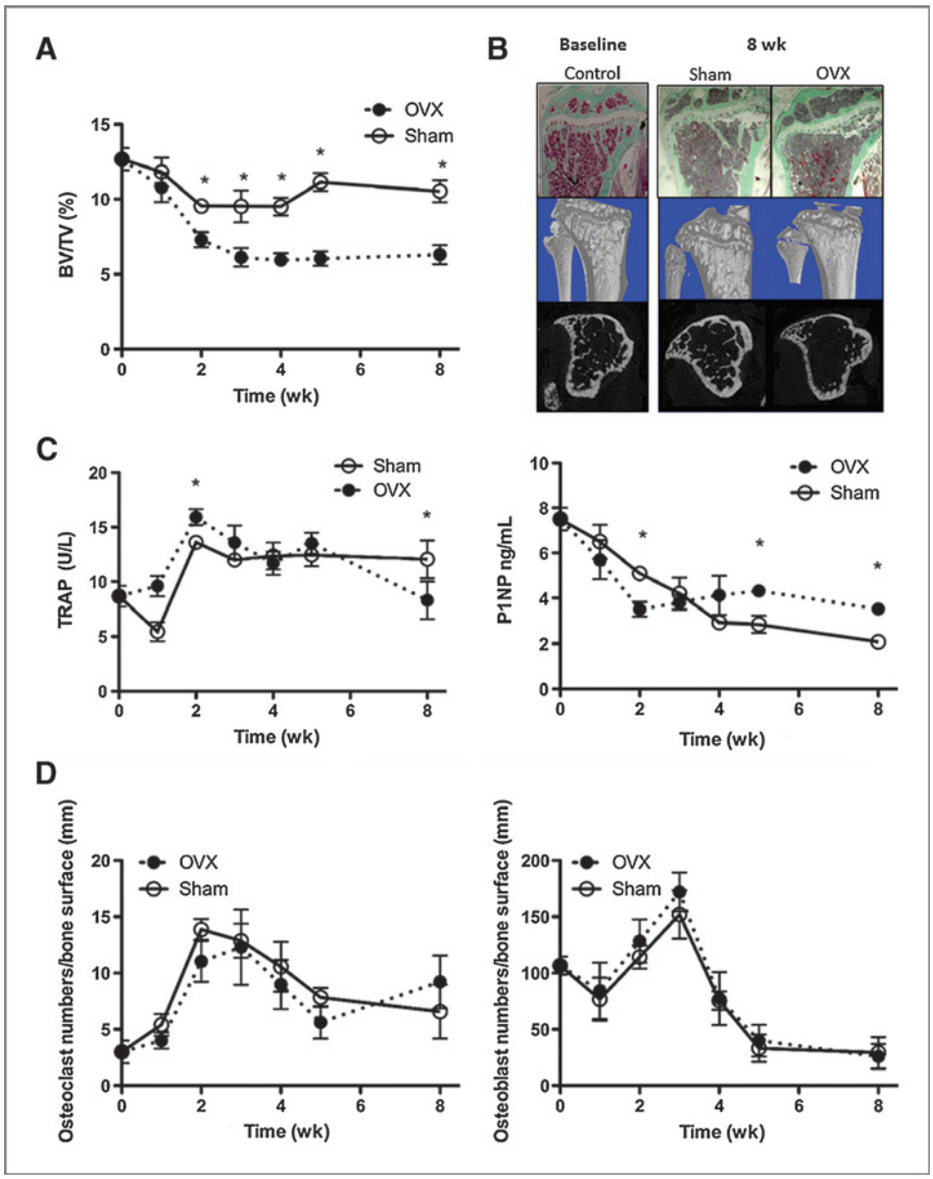

Figure 1. Effects of OVX on bone structure and bone turnover. A, bone volume 0, 1, 2, 3, 4, 5, and 8 weeks following OVX. B, photomicrographs of Goldners' stained histologic sections of the tibia and reconstructed micro-CT images at baseline and 8 weeks following OVX or sham operation. C, osteoclast activity was analyzed by measuring serum levels of TRACP 5b and osteoblast activity assessed by measuring P1NP in ovariectomized mice compared with sham-operated animals. D, numbers of osteoclasts and osteoblasts lining the bone surface 0, 1, 2, 3, 4, 5, and 8 weeks following OVX. Data, mean ± SEM; *, $P < 0.05$.

increased tumor cell colonization and/or ability of tumor cells to form overt colonies.

Effects of ovariectomy on growth of disseminated breast tumor cells in bone

Following intracardiac implantation of MDA-MB-231 cells in 12-week old animals, the majority of tumor cells that reach bone die within 72 hours, leaving behind a small number of disseminated tumor cells that do not form overt colonies. We investigated whether modifying the bone microenvironment through OVX affects the ability of these disseminated tumor cells to form colonies. OVX performed 7 days following tumor cell injection resulted in a substantial increase in tumor growth in bone, accompanied by a 34% and 36% loss in trabecular bone compared with the sham or control group, respectively ($P < 0.001$; Fig. 3). Of note, 89% of animals that had undergone OVX developed tumors in bone, compared with 17% of the animals in the control and 11% in the sham group ($P < 0.001$ for OVX vs. control or sham). Compared with the sham group, animals in the OVX group had both increased number (2.55 ± 0.86 tumors per long bone vs. 0.46 ± 0.32) and larger tumors (1.35×10^6 ± 0.02 p/s vs. 0.02 ± 0.01 p/s). The OVX-induced increase in tumor growth was specific to bone, with extraskeletal tumors detected in 18% of OVX, 17% of control, and 18% of sham-operated animals.

Differential effects of osteoclast inhibition on tumor growth in bone in the pre- and postmenopausal setting

We investigated whether tumor growth in bone was driven by increased bone resorption by treating sham and

Published OnlineFirst March 31, 2014; DOI: 10.1158/1078-0432.CCR-13-1246

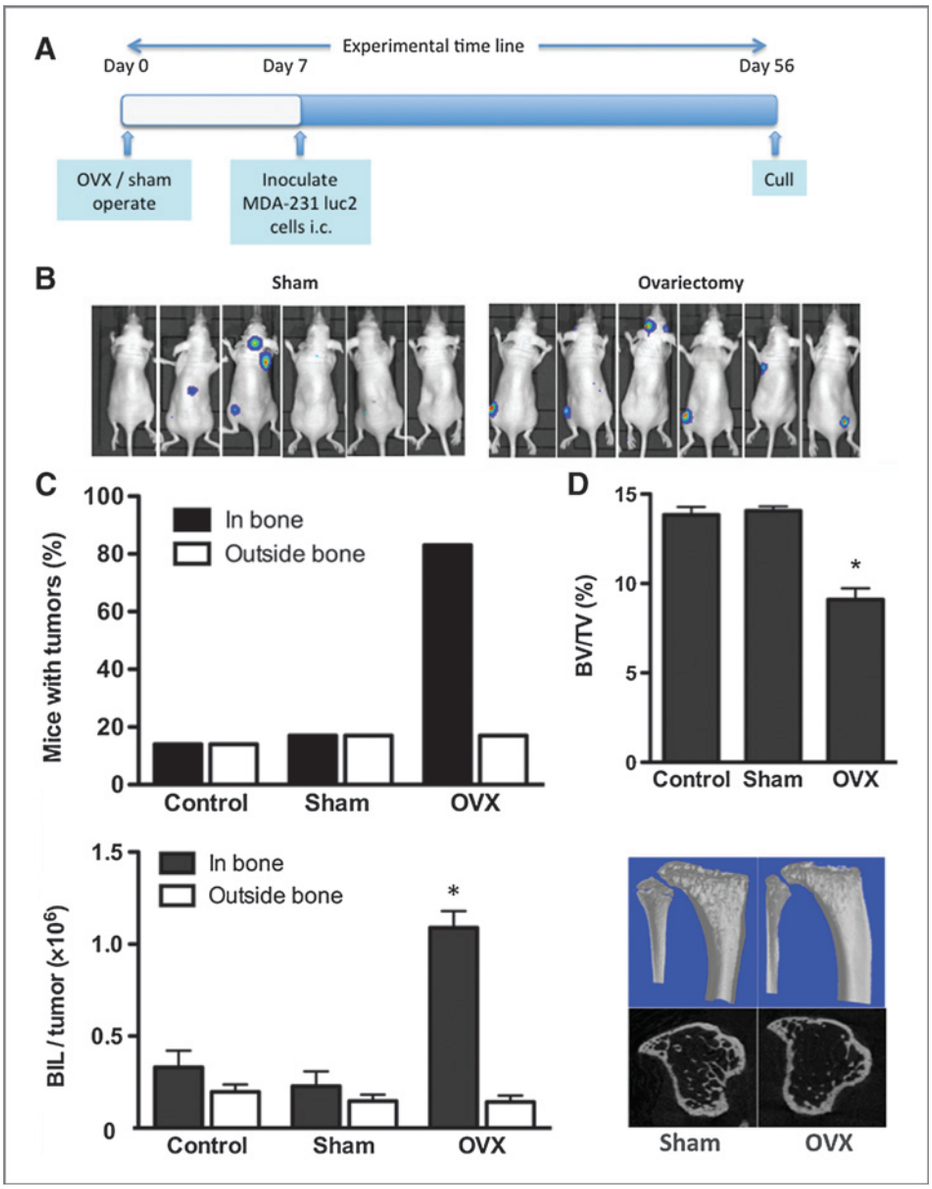

Figure 2. OVX increases of the number of MDA-MB-231 breast cancer cell colonies in bone. Experimental outline (A) and photographs (B) of luciferase-expressing MDA-MB-231 cells inoculated 7 days after OVX or sham operation and 56 days following tumor cell inoculation. The percentage of mice with detectable tumors and mean tumor volume ± SEM shown as numbers of p/s per tumor (C). Bone volume following OVX in mice injected with MDA-MB-231 cells (mean ± SEM) and micro-CT images representing bone architecture (D). All data are shown for 56 days following tumor cell inoculation; *, $P < 0.05$.

OVX animals with the potent osteoclast inhibitor ZOL. MDA-MB-231 cells were injected intracardially in two groups of animals that received weekly injections of saline (control, $n = 20$) or ZOL (100 μg/kg, $n = 20$) for 4 weeks. Half of the animals from each group subsequently underwent either a sham operation or OVX on day 7 ($n = 10$/group) and tumor growth was monitored until day 35. Of note, 86% animals that underwent OVX had detectable tumors in bone compared with 33% of sham ($P < 0.001$), supporting that increased bone resorption stimulated tumor growth in the postmenopausal setting (Fig. 4). There was a significant reduction of tumor growth in bone in OVX animals treated with ZOL (17%) compared with OVX control (86%; $P < 0.001$). In contrast, ZOL treatment did not affect skeletal tumor growth in the sham group, with 33% of both control and ZOL-treated sham-operated animals having detectable tumors in bone. Despite the differential effects on tumor growth, ZOL caused a significant increase in bone volume in both OVX and sham-operated animals compared with the respective controls (Fig. 4C and D). Bone volume/trabecular volume (BV/TV) increased from 12.91 ± 1.25% in sham OVX to 17.21 ± 1.15% in sham ZOL ($P < 0.01$) and from 10.52 ± 1.29% in OVX control compared with 16.25 ± 1.37% ($P < 0.01$), no significant differences in bone volume were detected between sham or OVX animals treated with ZOL, demonstrating that bone resorption is reduced to the same extent in models of pre- and postmenopausal bone.

Multiphoton microscopy confirmed the presence of individual MDA-MB-231 cells in the long bones of animals that had not developed overt bone tumors on day 35 regardless

Published OnlineFirst March 31, 2014; DOI: 10.1158/1078-0432.CCR-13-1246

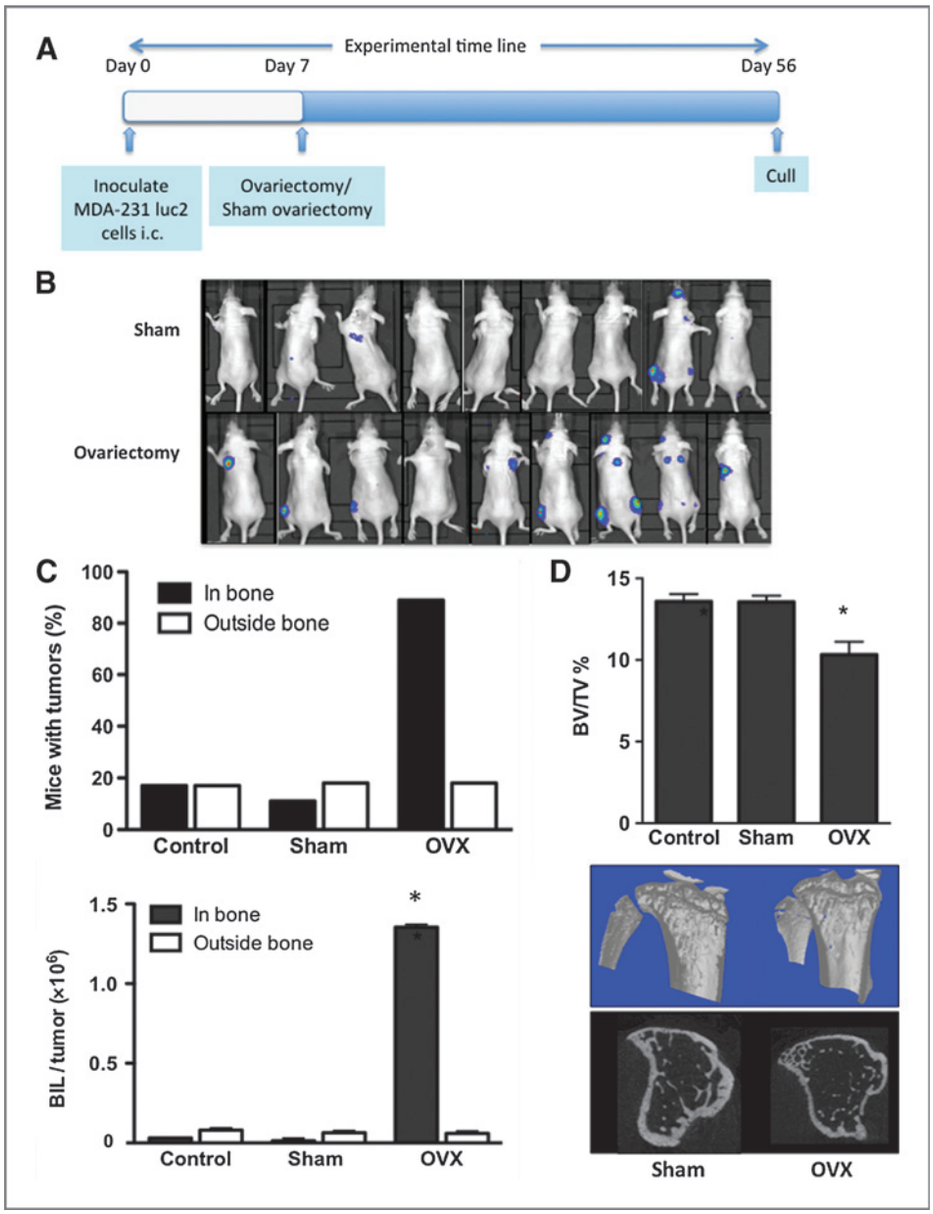

Figure 3. OVX stimulates growth of established breast cancer cells in long bones of 12-week-old immunocompromised mice. Experimental outline (A) and photographs of luciferase-expressing MDA-MB-231 cells inoculated 7 days before OVX or sham operation growing in mice 49 days following tumor cell inoculation (B). The percentage of mice with detectable tumors and mean tumor volume ± SEM is shown as numbers of p/s per tumor (C). Effects on bone volume following OVX in mice injected with MDA-MB-231 cells (mean ± SEM) and micro-CT images representing bone architecture (D). All data are shown for 49 days following tumor cell inoculation; *, $P < 0.05$.

of the group, demonstrating that the tumor cells successfully engrafted in bone but remained nonproliferative for extensive periods in all settings (Fig. 5).

OVX-induced gene expression changes in the bone microenvironment are modified by ZOL

We compared the expression of a panel of genes using long bones isolated from control and ZOL-treated animals 7 days following OVX or sham operation. The genes were selected on the basis of reported roles in bone turnover and/or tumor growth in bone, as well as stem cell mobilization. Table 1 shows the genes for which a more than 2-fold change in expression levels between OVX and sham was detected. A full gene list is given in Supplementary Table S2. As expected, OVX induced expression of a number of genes associated with increased bone resorption (including *cathepsin K, TRAP, MMP9, RANKL,* and *PTH*), which was inhibited by treatment with ZOL. There was a significant change in genes affecting bone formation following OVX (including reduced expression of the osteoblast formation inhibitors *Dkk1, 2* and *3*), and this was reversed in the ZOL-treated animals. ZOL-modified expression genes linked to bone turnover in both the sham and OVX animals, in agreement with the ability of ZOL to inhibit bone loss in both groups (Fig. 4). Interestingly, ZOL differentially modified genes associated with stem cell mobilization in sham and OVX animals.

Effects of PTH on MDA-MB-231 tumor growth in bone

Molecular analysis of bones from OVX-operated animals showed a significant increase in PTH expression compared

Published OnlineFirst March 31, 2014; DOI: 10.1158/1078-0432.CCR-13-1246

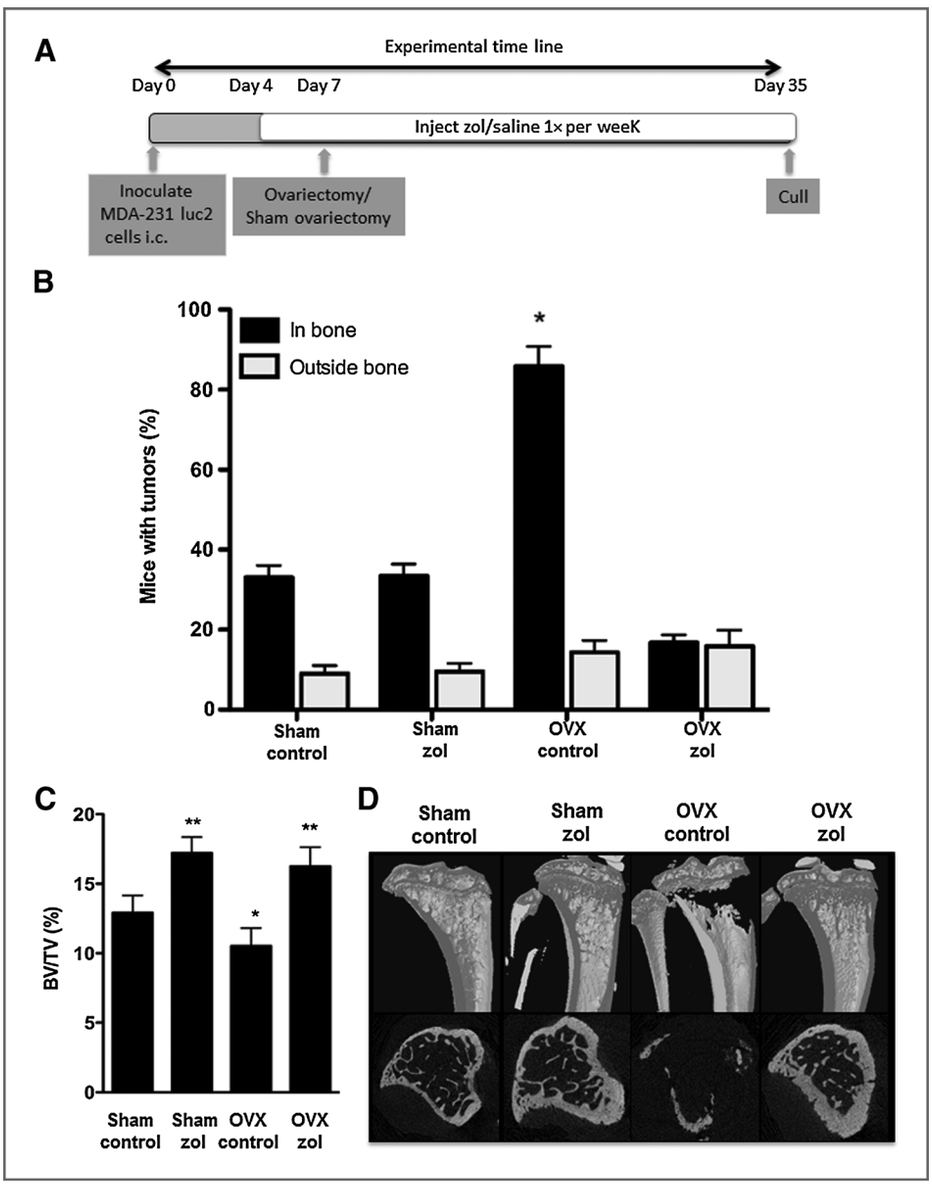

Figure 4. ZOL inhibits bone resorption and reduces tumor take in ovariectomized mice. A, experimental outline. B, histogram, mean ± SEM% of mice with detectable bone tumors in control and ZOL-treated ovariectomized and sham-operated mice 35 days following tumor cell inoculation. C, bone volume compared with trabecular volume 28 days following OVX and 31 days following ZOL treatment in mice preinjected with MDA-MB-231 cells (mean ± SEM). D, micro-CT images representing bone architecture at the end of the experimental protocol. *, $P < 0.05$ compared with sham control; **, $P < 0.05$ compared with sham control and OVX control.

with sham-operated animals, which was reversed by treatment with ZOL. Analysis of serum from OVX and sham-operated animals by ELISA showed a trend toward increased levels of PTH following OVX (12.82 ± 1.12 pg/mL) compared with control (16.31 ± 1.25) although this did not reach significance ($P = 0.055$, data not shown). We, therefore, investigated the effects of PTH on tumor growth in bone. Administration of 80 μg/kg rhPTH for 5 days resulted in a 29% increase in TRAP levels reflecting elevated osteoclast activity, accompanied by an increase in tumors from 0.6 per mouse in control to 2.14 per mouse in PTH-treated animals (Supplementary Fig. S3A and S3B). These data demonstrate a correlation between increased bone resorption and tumor growth in bone, similar to those obtained following OVX.

Discussion

Using experimental systems that separately model the pre- and postmenopausal bone microenvironment, combined with advanced imaging of disseminated tumor cells in bone, we have identified major differences in tumor growth and response to antiresorptive therapy. Breast cancer cells homed to the long bones following intracardiac inoculation in 12-week-old mice, but failed to progress to form overt tumors in the majority of animals unless preceded by OVX (Fig. 2). OVX also induced the growth of disseminated tumor cells in bone, whereas a sham operation did not (Fig. 3). We used the established estrogen-independent MDA-MB-231 cells, as estrogen-dependent MCF7 cells did not form bone metastasis following intracardiac injection 10 weeks after implantation (data not

Published OnlineFirst March 31, 2014; DOI: 10.1158/1078-0432.CCR-13-1246

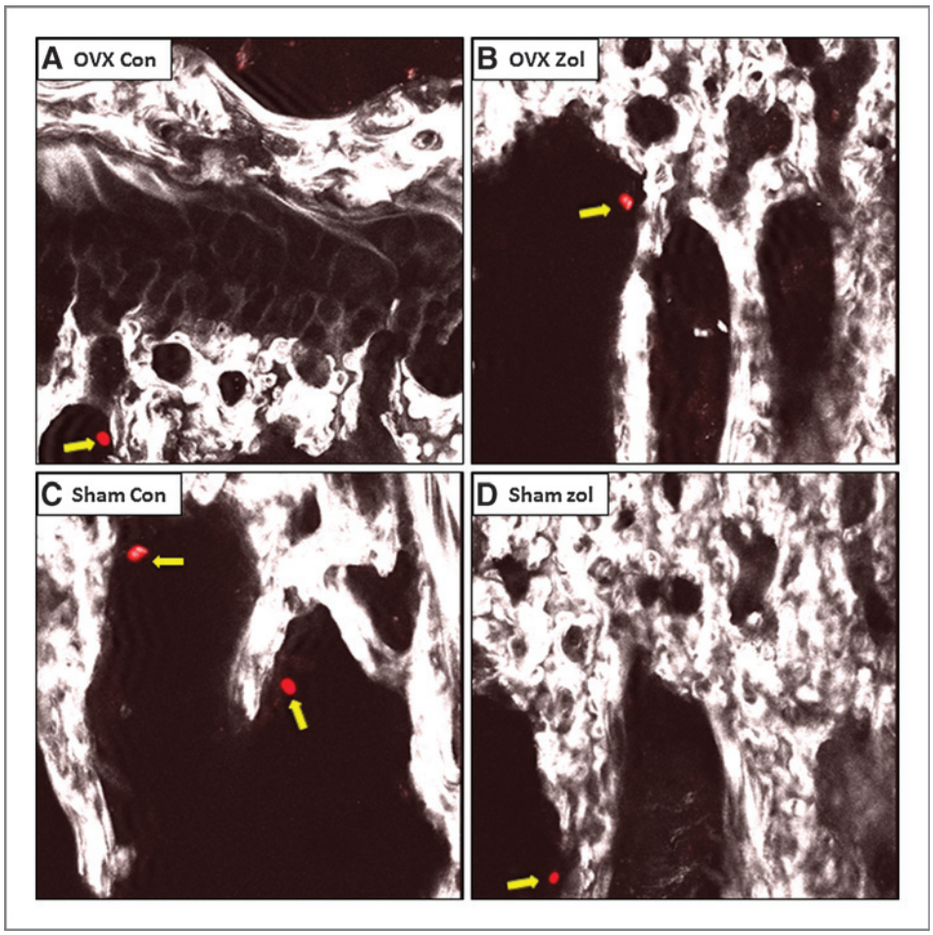

Figure 5. Nonproliferating tumor cells are present in proximal trabecular bone of mice without detectable metastasis. Confocal images of disseminated DiD-labeled tumor cells (red cells highlighted with yellow block arrows) that have homed to bone but not formed tumors in tibiae of ovariectomized control mice (A), ovariectomized ZOL-treated mice (B), sham control (C), and sham ZOL-treated animals (D).

shown). Estrogen supplementation caused major changes to the bone volume structure significantly altering the bone microenvironment and, hence, was unsuitable for our studies (Supplementary Fig. S4).

A limitation of our study is the differences in bone turnover rates in mice and humans, with changes to the bone microenvironment following OVX manifesting themselves within a few days in mice. These rapid changes may affect the growth of resident tumor cells to a higher degree than would be the case in humans. However, as early stages of tumor cell colonization of bone cannot be studied in patients, model systems continue to provide valuable information relating to initiation of bone metastasis. ZOL specifically inhibited OVX-induced bone tumor growth, supporting the observed benefit of anti-resorptive therapy in patients with postmenopausal breast cancer (1, 3). In contrast, no effect on tumor growth in bone was seen in sham-operated animals, reflecting the lack of benefit of adjuvant ZOL in the patients with premenopausal breast cancer (1, 13). Our results provide new insights into the mechanisms driving tumor growth in bone that may contribute to differential therapeutic effects of ZOL in the pre- and postmenopausal setting.

We present two major findings; first, that OVX-induced changes to the bone microenvironment can trigger growth of disseminated breast tumor cells, and second, that these changes are completely abolished by ZOL and, hence, mediated by osteoclast activity. Our data support that tumor cells remain quiescent in the mature skeleton until they receive microenvironmental signals that stimulate their proliferation. Tumor cells that persist in bone are thought to occupy specific niches identical to, the hematopoietic stem cell (HSC) niche (7). Tumor proliferation in bone may, therefore, be regulated by many of the same processes that control HSC mobilization and quiescence, including osteoblast and osteoclast activities (14–16). Although not clearly defined, the "bone metastatic niche" maybe located at endosteal bone surfaces in the long bones. In agreement, the single tumor cells we detected in bone were closely associated with endosteal surfaces of trabecular bone in proximity to the growth plate (Fig. 5).

There is accumulating evidence that osteoclasts are central to mobilization of HSCs, mainly through the production of proteolytic enzymes that disrupt SDF-1–CXCR4 interactions (14). Increased bone resorption following administration of RANKL stimulates egress of HSCs from bone marrow niches into the circulation, disrupts the

Published OnlineFirst March 31, 2014; DOI: 10.1158/1078-0432.CCR-13-1246

Table 1. Genetic alterations in mouse long bone 1 week following OVX with and without ZOL treatment

	Protein coded for	Fold change OVX vs. Sham	Fold change Sham Zol vs. Sham	Fold change OVX Zol vs. Sham Zol	Fold change OVX Zol vs. OVX
KitL	C-kit ligand	5.33 ± 0.91[a]	−1.34 ± .56	4.23 ± 0.83[a]	−1.90 ± 0.11
Tnfsf11	Receptor activator of NK-κB ligand	4.87 ± 0.58[a]	−2.2 ± 0.12[a]	0.35 ± 0.97	−6.73 ± 1.26[a]
BGlap	Osteocalcin	4.69 ± 2.39[a]	4.96 ± 1.54[a]	5.83 ± 0.49[a]	5.74 ± 2.04[a]
Ctsk	Cathepsin K	3.81 ± 0.12[a]	−3.09 ± 0.63[a]	0.07 ± 0.23	−6.82 ± 0.38[a]
Spp1	Osteopontin	3.74 ± 0.51[a]	−2.06 ± 0.38	0.07 ± 0.44	−5.74 ± 0.52[a]
Dkk1	Dickkopf 1	3.73 ± 0.69[a]	−2.86 ± 0.62[a]	0.18 ± 0.49	−6.42 ± 0.33[a]
Igf2	Insulin-like growth factor 2	3.71 ± 0.45[a]	0.36 ± 1.82	3.54 ± 1.36[a]	−0.07 ± 0.66
MmP9	Matrix metallopeptidase 9	3.54 ± 0.41[a]	−2.11 ± 0.22	0.24 ± 0.11	−5.40 ± 0.22[a]
Lif	Leukemia inhibitory factor	3.36 ± 0.54[a]	1.06 ± 1.15	2.22 ± 0.31[a]	−0.36 ± 0.72
Cxcl12	Chemokine ligand 12	2.97 ± 0.73[a]	−1.65 ± 0.86	0.30 ± 0.19	−6.23 ± 1.51[a]
Dkk2	Dickkopf 2	2.96 ± 0.26[a]	−2.60 ± 0. 42[a]	0.27 ± 1.02	−5.30 ± 0.42[a]
Sp7	Osterix	2.91 ± 0.44[a]	0.18 ± 0.23	2.95 ± 0.98	0.22 ± 0.09
Igf1	Insulin-like growth factor 1	2.81 ± 0.25[a]	0.28 ± 0.43	2.39 ± 0.26[a]	−0.14 ± 0.19
MmP14	Matrix metallopeptidase 14	−2.77 ± 0.23[a]	−0.89 ± 0.71	−2.50 ± 0.41[a]	−0.61 ± 0.10
Tnf	Tumor necrosis factor	2.73 ± 0.16[a]	−2.57 ± 0.51[a]	0.37 ± 0.68	−4.91 ± 0.40[a]
Tnfrsf11b	Osteoprotegrin	−2.56 ± 0.11[a]	2.87 ± 0.53[a]	−0.44 ± 0.51	5.00 ± 0.72[a]
Dkk3	Dickkopf 3	2.46 ± 0.36[a]	−0.58 ± 0.64	0.08 ± 0.65	−3.99 ± 0.51[a]
MmP2	Matrix metallopeptidase 2	−2.35 ± 0.19[a]	2.72 ± 0.29[a]	−0.17 ± 0.35	4.90 ± 0.16[a]
Ccnd1	Cyclin D1	−2.31 ± 0.41[a]	−4.13 ± 0.56[a]	−0.38 ± 0.52	−4.51 ± 0.72[a]
Pth	Parathyroid hormone	2.26 ± 0.26[a]	0.09 ± 0.87	−0.61 ± 0.71	−3.68 ± 1.57[a]
Apc5	TRAP	2.25 ± 0.22[a]	−2.43 ± 0.25[a]	0.15 ± 0.26	−5.13 ± 0.25[a]

[a]A *P* value of <0.05.

adhesion of HSCs and niche components that maintain cell quiescence resulting in proliferation (17). Other "stress" signals in the endosteal niche, for example, OVX-induced bone loss, may have similar effects. Remodeling of the extracellular matrix during bone resorption may also disrupt integrin interactions that maintain tumor cells in a state of quiescence (18).

Previous studies addressing the long-term skeletal effects of OVX in mouse models, show significant bone loss persisting for several weeks (19, 20). To capture the events associated with induction of disseminated tumor cell proliferation, we investigated the molecular and cellular changes to the bone microenvironment 7 days after OVX/sham operations. At this point, a range of genetic changes reflecting increased bone resorption and/or reduced bone formation were detectable (Table 1). OVX induced a significant increase in expression of *RANKL*, a stimulator of osteoclast formation and activity (21), coupled with decreased expression of the *RANKL* inhibitor osteoprotegerin (22). In addition, *Dkk-1*, an inhibitor of osteoblast differentiation was increased (23). OVX also caused increased expression of proteolytic enzymes associated with elevated osteoclast activity, including *MMP-9* and cathepsin K (24). In addition to the established roles in bone turnover, these molecules also activate the bone marrow endosteal stem cell niche and stimulate mobilization of vasculogenic progenitors (25). *MMP9* plays a critical role in mobilization of hematopoietic and endothelial precursor cells from the bone marrow niche through cleaving of membrane KITL to its soluble form, a key component of the osteoblast stem cell niche essential for endosteal lodging of murine stem cells (24). Interestingly, *c-KitL* was the gene most upregulated following OVX. It is possible that changes in the levels of *cKitL* may also affect the mobilization of tumor cells that reside in the niche. We hypothesize that the nonproliferating tumor cells present in the bone marrow before OVX are the cells that have the capacity to form tumors and, hence, have stem cell–like properties, and modification of the bone microenvironment mediates mobilization of these cells from bone marrow niches and initiates tumor growth. Importantly, the increased tumor growth following OVX was not a result of increased numbers of tumor cells homing to bone compared with sham (Supplementary Fig. S2).

We used the antiresorptive agent, ZOL, to establish whether OVX-induced tumor growth was triggered by increased osteoclast activity. ZOL increased bone volume to the same extent in animals that had undergone either sham or OVX, reflected by changes in bone gene expression levels. These results are in agreement with clinical studies showing that ZOL decreases the level of bone resorption markers in both pre- and postmenopausal women (1, 13). However, we found major differences in the ability of ZOL to modify tumor growth in bone. In the sham group,

Published OnlineFirst March 31, 2014; DOI: 10.1158/1078-0432.CCR-13-1246

mimicking the premenopausal setting, ZOL had no effect on the growth of skeletal tumors (Fig. 4). In contrast, ZOL completely prevented OVX-induced tumor growth in bone (mimicking the postmenopausal setting). Only four genes (*KitL*, *Igf1*, *Igf2*, and *MmP14*) in our panel were differentially affected by ZOL in the OVX versus the sham group, all of which are associated with regulating stem cell niches (26–28). Further studies are required to establish the role of these changes in initiation of bone metastasis. Tumor growth outside the skeleton (including lung) was not affected by ZOL treatment in either group, but the models do not capture metastasis to extraskeletal sites that may occur during subsequent tumor progression. We have previously shown that administration of 100 μg/kg ZOL weekly for 6 weeks does not induce tumor cell apoptosis in a bone metastasis model; hence, ZOL does not reduce tumor growth by direct tumor cell toxicity (29). There are clear limitations to mimicking effects of menopause in mice, in particular the role of the changes in circulating hormones. However, our results clearly indicate that breast tumor progression in bone involves different mechanisms in the pre- and postmenopausal microenvironment, and that it may potentially only be driven by osteoclast activity in postmenopausal bone.

Our data are the first to demonstrate that the cellular and molecular mechanisms are responsible for driving tumor growth differ in the pre- (sham) and postmenopausal (OVX) bone metastasis models. We show that osteoclast-mediated mechanisms are instrumental for the progression of disseminated tumor cells in bone only in the postmenopausal model and, hence, provide biologic evidence underpinning why the benefit of adjuvant antiresorptive therapy reported is restricted to patients with postmenopausal breast cancer in recent clinical trials.

Disclosure of Potential Conflicts of Interest

P.I. Croucher reports receiving a commercial research grant from Novartis Pharma. No potential conflicts of interest were disclosed by the other authors.

Authors' Contributions

Conception and design: P.D. Ottewell, P.I. Croucher, C.L. Eaton, I. Holen
Development of methodology: P.D. Ottewell, N. Wang, K.J. Reeves
Acquisition of data (provided animals, acquired and managed patients, provided facilities, etc.): P.D. Ottewell, N. Wang, H.K. Brown, C.A. Fowles
Analysis and interpretation of data (e.g., statistical analysis, biostatistics, computational analysis): P.D. Ottewell, C.A. Fowles, P.I. Croucher, I. Holen
Writing, review, and/or revision of the manuscript: P.D. Ottewell, N. Wang, P.I. Croucher, C.L. Eaton, I. Holen
Administrative, technical, or material support (i.e., reporting or organizing data, constructing databases): P.D. Ottewell, C.A. Fowles
Study supervision: P.D. Ottewell, P.I. Croucher, C.L. Eaton, I. Holen

Acknowledgments

The authors thank Orla Gallagher and Darren Lath who provided expert bone processing and sectioning.

Grant Support

This study was supported by a program grant from Cancer Research UK (to C.L. Eaton, P.I. Croucher, and I. Holen). P.I. Croucher is supported by Janice Gibson and the Ernest Heine Family Foundation.

The costs of publication of this article were defrayed in part by the payment of page charges. This article must therefore be hereby marked *advertisement* in accordance with 18 U.S.C. Section 1734 solely to indicate this fact.

Received May 9, 2013; revised December 18, 2013; accepted March 4, 2014; published OnlineFirst March 31, 2014.

References

1. Coleman RE, Marshall H, Cameron D, Dodwell D, Burkinshaw R, Keane M, et al. Breast cancer adjuvant therapy with zoledronic acid. N Engl J Med 2011;365:1396–405.
2. Paterson AHG, Anderson SJ, Lembersky BC, Fehrenbacher L, Falkson CI, King KM, et al. NSABP protocol B-34: a clinical trial comparing adjuvant clodronate vs. placebo in early stage breast cancer patients receiving systemic chemotherapy and/or tamoxifen or no therapy—final analysis. Cancer Res 2011;71(24 Suppl): S2–3.
3. Gnant M, Mlineritsch B, Stoeger H, Luschin-Ebengreuth G, Heck D, Menzel C, et al. Adjuvant endocrine therapy plus zoledronic acid in premenopausal women with early-stage breast cancer: 62-month follow-up from the ABCSG-12 randomised trial. Lancet Oncol 2011;12:631–41.
4. Townson JL, Chambers AF. Dormancy of solitary metastatic cells. Cell Cycle 2006:16:1744–50.
5. Aguirre-Ghiso JA. Models, mechanisms, and evidence for cancer dormancy. Nat Rev Cancer 2007;7:834–846.
6. Weilbaecher KN, Guise TA, McCauley L. Cancer to bone: a fatal attraction. Nat Rev Cancer 2011;11:411–25.
7. Shiosawa Y, Pedersen EA, Havens AM, Jung Y, Mishra A, Joseph J, et al. Human prostate cancer metastases target the hematopoietic stem cell niche to establish footholds in mouse bone marrow. J Clin Invest 2011;121:1298–312.
8. van der Pluijm G, Que I, Sijmons B, Buijs JT, Löwik CW, Wetterwald A, et al. Interference with the microenvironmental support impairs the de novo formation of bone metastases *in vivo*. Cancer Res 2005;65: 7682–90.
9. Brown HK, Holen I. Antitumour effects of bisphosphonates—what have we learned from *in vivo* models? Current Cancer Drug Targets 2009;9:807–23.
10. Ottewell PD, Mönkkönen H, Jones M, Lefley DV, Coleman RE, Holen I. Antitumor effects of doxorubicin followed by zoledronic acid in a mouse model of breast cancer. J Natl Cancer Inst 2008;100:1167–78.
11. Cole AA, Walters LM. Tartrate-resistant acid phosphatase in bone and cartilage following decalcification and cold-embedding in plastic. J Histochem Cytochem 1987;35:203–6.
12. Parfitt AM, Drezner MK, Glorieux FH, Kanis JA, Malluche H, Meunier PJ, et al. Bone histomorphometry: standardization of nomenclature, symbols, and units. Report of the ASBMR Histomorphometry Nomenclature Committee. J Bone Miner Res 1987;2:595–610.
13. Steinman EA, Brufsky AM, Oesterreich S. Zoledronic acid effectiveness against breast cancer metastases—a role for oestrogen in the microenvironment? Breast Cancer Res 2012;14:213.
14. Kollet O, Dar A, Lapidot T. The multiple roles of osteoclasts in host defence: bone remodelling and hematopoietic stem cell mobilisation. Annu Rev Immunol 2007;25:51–69.
15. Renstrom J, Kroger M, Peschel C, Oostendorp RAJ. How the niche regulates hematopoietic stem cells. Chem Biol Interact 2010;184:7–15.
16. Ellis SL, Grassinger J, Jones A, Borg J, Camenisch T, Haylock D, et al. The relationship between bone, hemopoietic stem cells, and vasculature. Blood 2011;11:1516–24.
17. Kollet O, Dar A, Shivtiel S, Kalinkovich A, Lapid K, Sztainberg Y, Tesio M, et al. Osteoclasts degrade endosteal components and promote mobilisation of hematopoietic progenitor cells. Nat Med 2006;12: 657–64.

Published OnlineFirst March 31, 2014; DOI: 10.1158/1078-0432.CCR-13-1246

18. Barkan D, Green JE, Chambers AF. Extracellular matrix: a gatekeeper in the transition from dormancy to metastatic growth. Eur J Cancer 2010;46:1181–8.
19. Lee SK, Kadono Y, Okada F, Jacquin C, Koczon-Jaremko B, Gronowicz G, et al. T lymphocyte-deficient mice lose trabecular bone mass with ovariectomy.J Bone Miner Res 2006;21:1704–12.
20. Orlić I, Borovecki F, Simić P, Vukicević S. Gene expression profiling in bone tissue of osteoporotic mice. Arh Hig Rada Toksikol 2007;58:3–11.
21. Lacey DL, Timms E, Tan HL, Kelley MJ, Dunstan CR, Burgess T, et al. Osteoprotegerin ligand is a cytokine that regulates osteoclast differentiation and activation. Cell 1998;93:165–76.
22. Simonet WS, Lacey DL, Dunstan CR, Kelley M, Chang MS, Lüthy R, et al. Osteoprotegerin: a novel secreted protein involved in the regulation of bone density. Cell 1997;89:309–19.
23. Van der Horst G, van der Werf SM, Farih-Sips H, van Bezooijen RL, Löwik CW, Karperien M. Downregulation of Wnt Signalling by increased expression of Dkckkopf-1 and -2 is a prerequisite for late stage osteoblast differentiation of KS483 cells. J Bone Mineral Res 2005;20:1867–77.
24. Jodele S, Blavier L, Yoon JM, DeClerck YA. Modifying the soli to affect the seed: role of stromal-derived matrix metalloproteinases in cancer progression. Cancer Metastasis Rev 2006;25:35–43.
25. Aicher A, Kollet O, Heeschen C, Liebner S, Urbich C, Ihling C, et al. the Wnta antagonist Dickkopf-1 mobilises vasculogenic progenitor cells via activation of the bone marrow enodstal stem cell niche. Circ Res 2008;103:796–803.
26. Driessen RL, Johnston HM, Nilsson SK. Membrane bound stem cell factor is a key regulator in the initial lodgement of stem cells within the endosteal marrow region. Exp Hematol 2003;31:1284–91.
27. Kumar S, Ponnazhagan S. Mobilization of bone marrow mesenchymal stem cells *in vivo* augments bone healing in a mouse model of segmental bone defect. Bone 2012;50:1012–8.
28. Lu C, Li XY, Hu Y, Rowe RG, Weiss SJ. MT1-MMP controls human mesenchymal stem cell trafficking and differentiation. Blood 2010; 14:221–229.
29. Ottewell PD, Woodward JK, Lefley DV, Evans CA, Coleman RE, Holen I. Anticancer mechanisms of doxorubicin and zoledronic acid in breast cancer tumor growth in bone. Mol Cancer Ther 2009;8:2821–32.